Phase-space dynamics of Bose condensates: Interference versus interaction

H. Wallis, A. Röhrl, M. Naraschewski, and A. Schenzle
Max-Planck-Institut für Quantenoptik, Hans-Kopfermann-Straße 1, D-85748 Garching, Germany
and Sektion Physik, Ludwig-Maximilians-Universität München, Theresienstraße 37, D-80333 München, Germany
(Received 11 September 1996)

We study theoretically the macroscopic interference of two independent Bose condensates released from a double potential trap. The observation of fringes could serve as a test for the paradigm of broken gauge symmetry. By numerical solution of the nonlinear Schrödinger equation in three dimensions, the consecutive stages of expansion, overlap, and interference are investigated in order to facilitate the design of future experiments. The phase-space dynamics of the condensates is analyzed by means of the Wigner function. It turns out that the distance of interference fringes grows linearly in time with a velocity inversely proportional to the initial distance of the two condensates. The collisional reduction of the fringe visibility is estimated. [S1050-2947(97)09502-4]

PACS number(s): 03.75.Fi, 05.30.Jp

I. INTRODUCTION

In view of the recent progress in preparing Bose condensed ultracold atomic gases [1,2], the question of interference of Bose condensates is of fundamental interest. The interference of independent atomic sources appears to be the most convincing manifestation of a so-called macroscopic wave function corresponding to the broken gauge symmetry in Bose-Einstein condensation. This effect has been shown previously only by the Josephson interference of superconducting currents. By comparison with condensed matter systems, the physics of dilute atomic gases is in much closer agreement with the perturbative theory of the atom-atom interactions. This fact makes quantitative simulations of experiments possible and attractive.

The notion of broken gauge symmetry or the existence of a macroscopic wave function, i.e., a nonvanishing ensemble average of the field operator $\langle \hat{\psi}(x) \rangle \neq 0$, proved to be an extremely useful concept in describing phase transitions in degenerate quantum liquids. Strictly speaking, however, breaking of gauge invariance requires breaking of particle conservation and can therefore be formulated consistently only in the thermodynamic limit. In view of the small atom numbers collected in atomic traps, the applicability of such a concept is not immediately obvious. It seemed particularly puzzling that interference phenomena as predicted in a classical field theory should be observed for fixed atom number N since a definite relative phase between independent condensates cannot be assumed. The incompatibility between these two views could recently be resolved by the investigation of correlation functions [3,4], which is the natural approach since it is the correlation that is observed experimentally. Interference fringes between condensates with *finite* particle number can be expected in single runs of the experiments even though the average over many runs does not show fringes. An analysis of such a situation in terms of continuous measurement theory [5] has shown in addition that only the distribution of the relative phase between the condensates undergoes spontaneous breaking of the gauge symmetry due to the measurement. This reflects the fact that although the total number of particles is altered by the measurement in a definite way, its distribution among the two condensates becomes more and more uncertain [6,7].

More generally, the notion of spontaneously broken gauge symmetry should be replaced [4] by a suppressed decay of multitime correlation functions of the condensate modes, of the form $\langle a^{\dagger}(t) a(t+\tau) \rangle$. Although a vanishing decay of this correlation is assumed in the thermodynamic limit, no reliable quantitative results are known up to now to determine its behavior in a finite system in the presence of interactions. An answer to this question might be obtained by the current experiments and is of utmost importance for the envisioned use of a Bose condensate as a coherent source of atoms.

We have already proposed in [4] to address the question of coherence experimentally by studying the interference of two independent Bose condensates. Visibility of these fringes (''high phase stability'') requires a negligible decay of the above correlation function for the experimental observation time τ.

A major obstacle to the experimental accessibility of the fringe pattern is the limited spatial resolution. For example, it was shown in [4] that fringes that might have existed in a previous double-trap experiment of Ketterle [1] would have been much narrower than the optical resolution of 8 μm. It is therefore one goal of this paper to develop a more detailed insight into the fringe formation in finite physical systems. This insight could facilitate the optimization of the experimental setup so as to achieve fringes of an observable size. It turns out that it should be possible, given the technology of current experiments, to achieve fringe periods larger than 10 μm, provided that the decay of the correlation is sufficiently slow. In addition, our predictions should help to discern expected fringes from possible other oscillatory density variations of the atomic clouds.

Interference with finite Bose condensed ensembles is holding great promise for new matter wave interferometers. Of course, matter wave interference with highly populated quantum states depends heavily on particle-particle interactions. While such interactions, for instance, vanish for coherent light waves interfering in vacuum, they cannot be removed for coherent matter waves. Even though the atom-

atom interactions in gases are weak compared to those in all other Bose condensed systems studied up to now, they turn out to be still strong enough to change the dynamics substantially compared to the noninteracting case.

In this paper we treat the interactions in the mean-field approximation, neglecting finite-temperature and dissipative effects. Propagation, overlap, and interference of two independent Bose condensates released from two minima of an optically plugged magnetic trap are well described by simulations of the nonlinear Schrödinger equation (NLSE). Unlike hydrodynamical similarity solutions based on the Thomas-Fermi approach [8,9], the NLSE is capable of describing the purely wave mechanical effect of interference.

The expansion of the cloud before and during the interference depends on the initial confinement and geometry of the sample. For large initial separation of the condensates the potential energy is completely transformed into kinetic energy before the condensates overlap. In an anisotropic configuration, the more rapid transverse expansion of the condensate reduces the nonlinearity of the evolution quickly. Most of our numerical results apply for conditions where the interactions thus play only a minor role during the formation and expansion of the fringes. In this regime we found that the fringe period grows in time with a velocity inversely proportional to the distance of the two condensates. The above situation is currently realized in the Ioffe trap experiments at MIT [10] and at JILA, Boulder.

The outline of the paper is as follows. In Sec. II, the interference of two Gaussian wave packets is presented in terms of Wigner functions, neglecting interactions. The time dependence of the spacing between consecutive interference fringes is derived. In Sec. III, the time-dependent nonlinear Schrödinger equation is applied to study the interplay of interference and interaction in the propagation of two overlapping condensates. The full three-dimensional treatment of a nonsymmetric propagation necessitates the use of some factorization methods for the NLSE. The comparison with a fully numerical treatment in two dimensions and with the predictions for noninteracting atoms is carried out. In Sec. IV, we discuss the dynamics of a single dense atom cloud, dominated by nonlinear effects. In the initial stage, the nonlinearity results in a slow adjustment of the wave function to the temporally varying external potentials. We finally discuss the limitation of the present description by collisionally induced decoherence in Sec. V.

II. INTERFERENCE OF NONINTERACTING ATOMS IN PHASE SPACE

We start by presenting the propagation of two Gaussian wave packets centered at different points in one-dimensional space. Our purpose here is to calculate the spacing between interference maxima as a function of time and to provide a precise and informative visualization of the overlap and interference of the wave packets for later comparison with the case of interacting atoms. Next, we want to revisit the issue of the relative phase of the condensate as discussed in [4] for the case of propagating wave packets considered here.

In the case of two noninteracting, independent Bose condensates, consider an initial Fock state such that two orthogonal states having the mode functions $u_1(x)$ and $u_2(x)$ are populated by N_1 and N_2 identical bosonic atoms. The many-particle wave function is simply written as $|N_1,N_2\rangle$. It is a straightforward extension of the work in [4] to show that the density distribution, seen in a single run of such an experiment, is besides some unavoidable shot noise given by

$$n_\phi(x,t)=N|\psi_\phi(x,t)|^2 \quad (N=N_1+N_2)$$

with

$$\psi_\phi(x,t)=\sqrt{\frac{N_1}{N}}u_1(x,t)+e^{i\phi}\sqrt{\frac{N_2}{N}}u_2(x,t). \tag{2.1}$$

Here ϕ is an equally distributed random phase variable that varies only between different runs of the experiment, and $u_{1,2}(x,t)$ are solutions of the linear Schrödinger equation with $u_{1,2}(x)$ as initial condition. In the absence of interactions all states $\psi_\phi(x,t)$ are degenerate. This many-particle interference is a truly quantum statistical effect and leads to fringes between the two condensates, with the spatial phase determined by the random value of ϕ.

In single-atom interference experiments, however, a single-atom wave function is coherently split up into two parts and spatially recombined later, thereby interfering with itself. The final wave function is then also described by Eq. (2.1), with N_i/N being replaced by the appropriate beam splitter ratio. The difference from the situation of independent condensates is that the relative phase ϕ is only determined by the geometry of the setup and does not change between different runs.

With these remarks in mind, we proceed to calculate the fringes arising for two freely expanding wave packets in the absence of interactions. In order to visualize the quantum interference, both in the absence and presence of interactions, the use of the familiar Wigner function [11] is well suited.

A second quantized form of the Wigner function would read

$$\hat{\mathcal{W}}(x,p)=\frac{1}{2\pi}\int dy\ e^{-ipy/\hbar}\hat{\psi}^\dagger\left(x-\frac{y}{2}\right)\hat{\psi}\left(x+\frac{y}{2}\right). \tag{2.2}$$

When a macroscopic wave function is employed to characterize a single run of the experiment, the corresponding Wigner function also has the single-particle form.

A. Fringe spacing for interfering Gaussian wave packets

Consider an initial one-dimensional wave function made of two Gaussian functions of equal amplitude centered at $\pm d$,

$$\psi(x)=\frac{1}{\sqrt{\mathcal{N}}}\left[\exp\left(-\frac{(x-d)^2}{2\sigma^2}\right)+\exp\left(-\frac{(x+d)^2}{2\sigma^2}+i\phi_s\right)\right], \tag{2.3}$$

with a free spatial phase ϕ_s. Here this phase is merely a parameter of the wave function. The normalization (allowing for overlap) reads $\mathcal{N}=\sqrt{\pi}2\sigma[1+\cos\phi_s\exp(-d^2/\sigma^2)]$, and the phase dependence of $\mathcal{N}$ vanishes for well separated condensates $\sigma\ll d$. The corresponding Wigner function reads

$$\mathcal{W}(x,p) = \frac{1}{2\pi}\int dy\, \exp(-ipy/\hbar)\,\psi\left(x+\frac{y}{2}\right)\psi^*\left(x-\frac{y}{2}\right)$$
$$= \frac{\exp\left(\frac{-p^2\sigma^2}{\hbar^2}\right)}{2\pi\left[1+\cos\phi_s\exp\left(-\frac{d^2}{\sigma^2}\right)\right]}\left(\exp\left(-\frac{(x-d)^2}{\sigma^2}\right)+\exp\left(-\frac{(x+d)^2}{\sigma^2}\right)+\underbrace{2\exp\left(-\frac{x^2}{\sigma^2}\right)\cos(2pd/\hbar-\phi_s)}_{\text{interference term}}\right) \tag{2.4}$$

In addition to the two peaks at $x=\pm d$, the initial Wigner function shows an interference pattern along the momentum axis with momentum period $\Delta p=\hbar\pi/d$, located at $x=0$. The central maximum of this pattern is shifted by the spatial phase ϕ_s. Neglecting interactions, the envelopes of all three terms are Gaussian. At time $t=0$, the interference pattern at $x=0$ does not contribute to the position density since its integral over momentum vanishes in the central zone. This interference zone is a clear feature of the nonlocal quantum nature of the initial phase space density, absent in the case of classical positive Gaussians [see Fig. 1(a)].

From the point of view of many-particle interference, the equal-time expectation value

$$\langle\hat{\mathcal{W}}(0,p)\rangle = \frac{1}{2\pi}\int dy e^{-ipy/\hbar}\left\langle\hat{\psi}^\dagger\left(-\frac{y}{2}\right)\hat{\psi}\left(\frac{y}{2}\right)\right\rangle \tag{2.5}$$

is some generalization of the so-called off-diagonal long-range order, conventionally characterizing broken symmetry in a Bose condensate. Remarkably, the notion of the ''phase of the condensate'' renders a straightforward, intuitive understanding of the capability to detect interference fringes in the present situation. Assuming broken U(1) symmetry for the states of the condensates, the spatial phase ϕ_s is *identified* with the relative phase of the two macroscopic wave functions of the condensate. The ensemble average performed in Eq. (2.5) corresponds to averaging over equally distributed phases in Eq. (2.4). The *phase-averaged* Wigner function shows no more correlations, the oscillations near $x=0$ vanish as well as the fringes in the position distribution for all later times.

During time evolution the initial distribution deforms and gives rise to a modulation of the position space density. The time evolution of noninteracting free atoms is given in phase space by the exact solution

$$\mathcal{W}(x,p,t) = \mathcal{W}(x-pt/m,p,0). \tag{2.6}$$

This is shown easily by considering the Liouville–von Neumann equation for the Wigner function. By Taylor expansion of this equation one proves the well-known result (see, e.g., [12]) that the motion of a particle in a potential $V(x)$ depends only on odd derivatives of the potential:

$$\left(\frac{\partial}{\partial t}+\frac{p}{m}\frac{\partial}{\partial x}\right)\mathcal{W}(x,p,t) = \sum_{\nu=0}^{\infty}\frac{\left(\frac{\hbar}{2i}\right)^{2\nu}}{(2\nu+1)!}\frac{\partial^{2\nu+1}V}{\partial x^{2\nu+1}}\frac{\partial^{2\nu+1}\mathcal{W}}{\partial p^{2\nu+1}}. \tag{2.7}$$

For classical particles, of course, only the $\nu=0$ term on the right-hand side contributes, and the classical Liouville equation is regained. For a single particle, the first quantum corrections occur only in the third-order terms [13]. This has the consequence that quantum and classical mechanics yield identical results for a linear or a quadratic potential, provided that the initial Wigner function is non-negative and can thus be interpreted as a classical phase space distribution. However, the Wigner function (2.4) is not completely amenable to a classical interpretation due to its interference term. The latter gives rise to nonclassical interference fringes in the position distribution when the two wave packets overlap.

Nevertheless, the *time evolution* of the Wigner function does obey in a certain sense ''classical mechanics.'' More precisely, during time evolution the initial interference zone is transformed into a linearly expanding fringe pattern according to Eq. (2.6). Equation (2.6) thus describes how a momentum distribution is turned into a position space distribution for time $t\to\infty$. Such measurements of the momentum distribution are actually performed in the expansion experiments [1,2,10].

One of the main results of this paper is the conclusion that the fringe spacing in *position* space increases with a velocity proportional to the initial fringe spacing Δp in *momentum* space,

$$v_{\text{fringe}} = \frac{\Delta p}{m} = \frac{\hbar\pi}{md}. \tag{2.8}$$

For a given time the spacing is thus inversely proportional to the distance between the initial wave packets. The fringes become visible in the position space density, obtained by integrating over the momentum p, when the expanding Gaussians overlap. This happens roughly at a time $\tau_0=md\sigma/\hbar$. At this time the first fringes with a spacing on the order of

$$\Delta p\,\tau_0/m = \sigma$$

become visible. This last result fortuitously coincides with an *a priori* guess that the fringe period should be related to the initial Gaussian momentum spread $\hbar/\sigma$. As the arguments

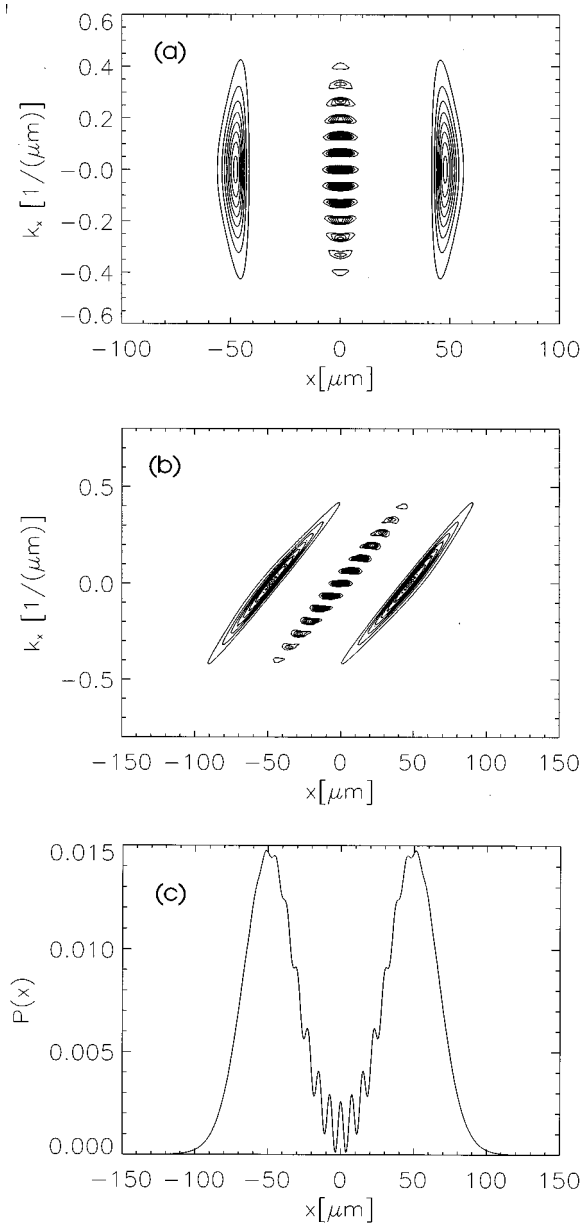

FIG. 1. Initial Wigner function for interfering wave packets in phase space. Only contours of the positive part are plotted for clarity. The momentum scale is given in wave vector units $k_x = p_x/\hbar$. The initial spatial separation is $d = 47$ μm and $\sigma = 4.1$ μm. The true ground state in the slightly asymmetric potential wells of the double Ioffe trap has been calculated numerically, neglecting interactions. The harmonic frequencies of the unperturbed Ioffe trap are 19 Hz and 250 Hz for the axial and transverse motion, maximum light shift $V_0 = h \times 25$ kHz, and beam waist of the laser beam $w_0 = 30$ μm. The interference region near $x = 0$ displays the fringes in the momentum distribution at $t = 0$ (a), which are transformed into fringes at a later time $t = 38.2$ ms (b). The fringes in position space are obtained by integrating over momentum in (b) and display well-resolved fringes in the position distribution (c).

are based only on Heisenberg's uncertainty relation (in the absence of interactions), it is solely the ratio of distance d and width σ that determines the number N_f of resolvable fringes at time τ_0,

$$N_f \propto d/\sigma.$$

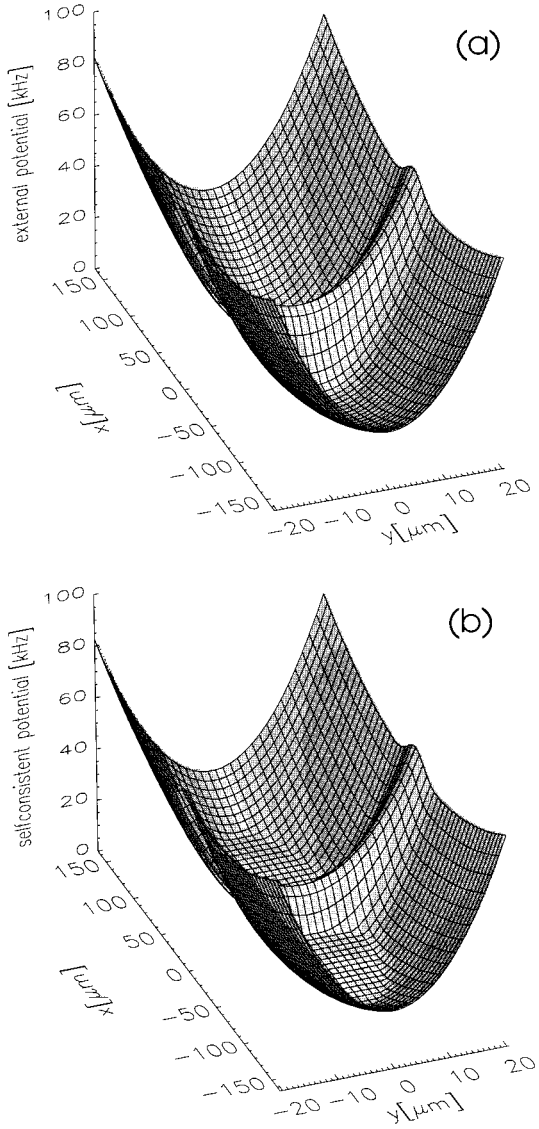

FIG. 2. (a) External potential of the double Ioffe trap, with the same parameters as in Fig. 1. (b) Self-consistent mean-field potential for interacting atoms. For a total atom number of $N = 5 \times 10^6$, the minima are still well separated.

However, these conclusions are modified through the interactions.

B. The case of the divided Ioffe trap

All of the above features can be recognized in Fig. 1. For the sake of comparison with the interacting case we have chosen a slightly different initial distribution, however. Instead of Gaussian wave packets, the initial state is the ground state of the external potential, as given by the experimental divided Ioffe trap employed by [14]. In the Ioffe configuration the atoms are collected in a cigar-shaped trap that is easily divided in two halves by a sheet of far-blue detuned, off-resonant laser light. The total potential is sketched in Fig. 2(a). The transverse and longitudinal frequencies are $\omega_x = 2\pi 19$ Hz and $\omega_{y,z} = 2\pi 250$ Hz, respectively. The asymmetry of the half traps is clearly reflected by the asymmetric Wigner function peaks at $x = \pm d$ in Fig. 1(a). The

central interference zone is plotted discarding the negative part of the Wigner function, for clarity. The linear deformation of the Wigner function due to the temporal evolution (2.6) is displayed in Fig. 1(b). Figure 1(c) shows the resulting position space interference fringes. The expansion has not yet produced complete overlap and the fringe spacing is still smaller than the initial width σ.

III. INTERFERENCE VERSUS INTERACTIONS

A. Mean-field description

In order to simulate the recent experiments [14] we now turn to the properties of interference under the influence of weak repulsive interactions. The dynamics of a trapped weakly interacting atomic gas is well described by Bogolyubov's formulation of the Hartree-Fock approximation for an atomic gas far below the condensation temperature [15]. To establish the fundamental physics involved we write down the effective grand canonical Hamiltonian

$$\hat{H}-\mu\hat{N}=\int d\mathbf{r}\ \psi^{\dagger}(\mathbf{r})(T+V-\mu)\psi(\mathbf{r}) + \frac{2\pi a\hbar^2}{m}\int d\mathbf{r}\ \psi^{\dagger}(\mathbf{r})\psi^{\dagger}(\mathbf{r})\psi(\mathbf{r})\psi(\mathbf{r}). \quad (3.1)$$

The effective δ-function interaction actually represents a properly renormalized two-particle interaction, i.e., a stands for the correct scattering amplitude. T represents the kinetic energy and V the trap potential. The standard procedure is to determine a stationary self-consistent wave function of the condensate by solving a nonlinear Schrödinger equation, the Gross-Pitaevski equation

$$\mu\psi(\mathbf{r})=\left(-\frac{\hbar^2\Delta}{2m}+V(\mathbf{r})+\widetilde{U}|\psi(\mathbf{r})|^2\right)\psi(\mathbf{r}), \quad (3.2)$$

with the chemical potential μ and

$$\widetilde{U}=\frac{4\pi\hbar^2 a}{m}. \quad (3.3)$$

For the time-dependent problem, the initial wave function is calculated from this equation. Based on the correlation function treatment of [4] it is a reasonable ansatz to describe also *two* independent condensates by one combined macroscopic wave function (2.1), for characterizing a single run of the experiment. The arbitrary relative phase φ between them is set to zero here.

In the usual perturbation theory, excitations out of the condensate are defined by splitting off a stationary expectation value $\hat{\psi}(\mathbf{r})=\psi(\mathbf{r})+\widehat{\delta\psi}(\mathbf{r})$. By contrast to this ansatz where $\psi(\mathbf{r})$ does not vary with time, we will explicitly allow for a *nonstationary* condensate wave function $\psi(\mathbf{r},t)$. The time evolution starts after the initial potential $V(\mathbf{r})$ is switched off, or modified, such that $\widetilde{V}(\mathbf{r})$ remains. In the time-dependent mean-field approximation we calculate the expansion and overlap of two independent condensates by solution of the NLSE,

$$i\hbar\frac{\partial}{\partial t}\psi(\mathbf{r},t)=\left(-\frac{\hbar^2\Delta}{2m}+\widetilde{V}(\mathbf{r})+\widetilde{U}|\psi(\mathbf{r},t)|^2\right)\psi(\mathbf{r},t). \quad (3.4)$$

Our simulation is based on the assumption that the initial state is a pure state and remains pure under the influence of the mean field for a sufficiently long time. We do not imply that the time evolution of the condensate does not give rise to excitations, but simply start from an initial state at zero temperature with no quasiparticles excited. Note that quasiparticle creation through collisions is slow for small atom densities and is not contained in the solution of the NLSE. For finite-temperature effects, i.e., the influence of noncondensate atoms in the initial state, we refer to [4]. There, the breakdown of the visibility has been shown for the noninteracting gas as the temperature approaches T_C.

B. Initial state

For an interacting atom cloud, the shape of the interference fringes will depend on the initial conditions, i.e., the initial confinement of the cloud due to the external potential. As a first approximation to the initial state we determine the so-called Thomas-Fermi solution of the Gross-Pitaevskii equation (3.2),

$$\rho(\mathbf{r},0)=\frac{\mu-V(\mathbf{r})}{\widetilde{U}}. \quad (3.5)$$

The external potential $V(\mathbf{r})$ in the double-trap configuration is displayed in Fig. 2(a). In the Thomas-Fermi approximation, the atomic density distribution mirrors the external potential, such that the self-consistent potential is flat, as is sketched in Fig. 2(b). It is apparent that for an atom number of $N=5\times10^6$, the sum of external and interaction potential still provides a suitable separation of the initial condensates, visible by the maximum in the middle of the trap. It is also apparent that the shape of the potential is not even nearly harmonic. To allow for the kinetic energy and obtain a more realistic initial condition, we have to replace the Thomas-Fermi solution by a numerical solution of the Gross-Pitaevskii equation. An efficient method to solve this problem is imaginary time propagation. By the substitution $\tau=it$ one obtains the imaginary time equation

$$\hbar\frac{\partial}{\partial\tau}\psi(\mathbf{r},\tau)=-\left(-\frac{\hbar^2\Delta}{2m}+V(\mathbf{r})+\widetilde{U}|\psi(\mathbf{r},\tau)|^2\right)\psi(\mathbf{r},\tau). \quad (3.6)$$

The lowest ''eigenstate'' of the nonlinear Hamilton operator on the rhs will have the smallest ''eigenvalue'' and thus survive temporal propagation, provided proper renormalizations of the amplitude are performed during propagation. Thus the ground state

$$\phi_0=\lim_{\tau\to\infty}\frac{\exp(-\tau H/\hbar)\psi}{||\exp(-\tau H/\hbar)\psi||} \quad (3.7)$$

is obtained from any initial wave function $\psi(0)$ with even parity. The solutions in Fig. 5(a) are obtained by this method.

C. Three-dimensional expansion of a single condensate

It is straightforward to characterize the time evolution of the condensates after switching off the trap as a ballistic expansion driven by the repulsive interaction energy stored in the trapped cloud. Its final free-flight stage is amenable to the simple phase space mechanics of Eq. (2.6) when the density has become low enough.

Previous studies of the expansion of interacting condensates have employed similarity solutions in order to describe the invariant features of the expanding cloud [8,9]. Such a solution is obtained by a scaling transformation of the initial distribution, reading here

$$\rho(\mathbf{r},t)=\overline{\lambda}^{-3}\rho(\Lambda(\mathbf{r},t),0) \tag{3.8}$$

with the map $\Lambda(\mathbf{r},t)=\Sigma_{i=1}^{3}\mathbf{e}_i[r_i/\lambda_i(t)]$ and $\overline{\lambda}^3(t)=\Pi_{i=1}^{3}\lambda_i(t)$ to be determined. After a short initial stage of the evolution the expansion is well described by an asymptotic linear scaling

$$\lambda_i(t)\rightarrow\tilde{\lambda}_i t. \tag{3.9}$$

The above ansatz can be combined with the so-called Thomas-Fermi solution, to give [8,9]

$$\rho(\mathbf{r},t)=\frac{\mu-\frac{m}{2}\sum_j \frac{\omega_j^2 r_j^2}{\lambda_j^2(t)}}{\tilde{U}\prod_j \lambda_j(t)}. \tag{3.10}$$

Equation (3.10) gives surprisingly good agreement with the experimentally measured distributions. While allowing for the interaction it neglects the wave mechanical nature of the center-of-mass motion, in the same way as Eq. (3.5), and is therefore not capable of describing interference fringes. The shape-invariant expansion of an initial Thomas-Fermi solution is correct in the case of a parabolic initial distribution. Higher order derivatives of the potential which might contribute to the Liouville equation (2.7) do not occur for the given quadratic shape of the potential.

In order to allow also for the interference, an exact solution of the NLSE must be sought. Only a direct numerical solution of the NLSE can both allow for the interference and provide evidence for the applicability of the scaling transform ansatz. A quantum-mechanical generalization of the scaling transform [9] does not avoid the inseparability of the three-dimensional NLSE. We therefore extend the one-dimensional NLSE to the three-dimensional case by using a factorization method. The factorization amounts to separating the mean-field Hamiltonian into a sum of Hamiltonians for each dimension $H=\Sigma_i H_i$, where

$$H_i=-\frac{\hbar^2}{2m}\frac{\partial^2}{\partial r_i^2}+V_i(r_i)+\tilde{U}|\psi_i(r_i)|^2\prod_{i\neq j}|\psi_j(r_{\max})|^2 \tag{3.11}$$

with the following product ansatz for the wave function:

$$\psi(\mathbf{r})=\prod_j \psi_j(r_j). \tag{3.12}$$

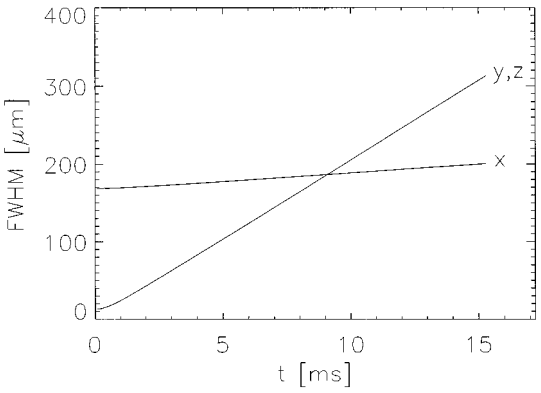

FIG. 3. Expansion of a single condensate after switching off the trap. We plot the axial (x) and transverse (y,z) diameter of the distribution calculated using the factorization approach. The data agree very well both with experimental data and with the scaling equations from [9]. Trap parameters are the same as in Fig. 1.

The nonlinearity is determined by the maximum density $|\psi_j(r_{\max})|^2$. Though deviations of the factorization ansatz become obvious for non-Gaussian wave functions, it turns out to yield the correct ratio of the expansion rates in the different directions. Thus we can keep the numerical effort tractable and still allow for the interference fringes which are not included in any Thomas-Fermi-type solution.

As a first test of the factorization scheme we have computed the expansion of a single condensate initially trapped in an anisotropic trap. By contrast to a thermal ensemble, the expansion continues to be anisotropic on the time scale of the observation. The calculated data (Fig. 3) display the circumstance that the extension in the direction of maximum compression overtakes the extension in the other directions at an early time, due to the steep initial density gradient in this direction. The results shown in Fig. 3 obtained from factorization agree with the prediction of the scaling equations for a cigar-shaped trap $\omega_y=\omega_z=\omega_\perp\gg\omega_x$,

$$\ddot{\lambda}_\perp=\frac{\omega_\perp^2}{\lambda_\perp^3\lambda_x},\quad \ddot{\lambda}_x=\frac{\omega_x^2}{\lambda_\perp^2\lambda_x^2}. \tag{3.13}$$

Second, to independently check the validity of the factorization we have also compared the separation ansatz with a solution allowing for two dimensions exactly and only factorizing a third degree of freedom. Besides the curvature, the general features of the nonlinear propagation seem to be well reproduced by the factorization approach [Fig. 4(a)]. However, by the two-dimensional calculation the correct two-dimensional curvature of the density contours is achieved [Fig. 4(b)]. For the calculation of the interference fringes the factorization approach is applicable as long as this curvature does not wash out the fringe pattern, when integrated over the transverse degrees of freedom. For the experimentally relevant parameters this is not the case.

D. Fringe spacing for interacting atoms

We now use the solutions of the NLSE to investigate the spatiotemporal structure of the evolving interference fringes in phase space. The purpose of using Wigner function plots is to facilitate the comparison of the data obtained by the

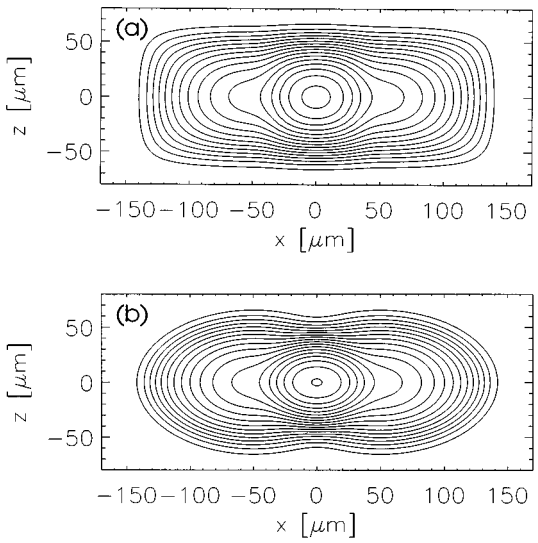

FIG. 4. Averaged density distribution of two overlapping condensates in the (x,z) plane, corresponding to the experimental situation of Ref. [2]. The interference structures were averaged out for better visibility of the effect of factorization. (a) The distribution as calculated using the factorization approach Eq. (3.12). (b) A two-dimensional solution of the NLSE, to be multiplied by a one-dimensional solution for the remaining degree of freedom, for the same parameters.

NLSE with the data for the noninteracting atoms. Recall that a freely expanding phase-space distribution undergoes a shearing deformation along the position axis (clockwise for our choice of coordinates). A rapid outward acceleration corresponds to a shearing deformation along the momentum axis (counterclockwise), while a deceleration is visualized as a shearing in the opposite sense.

Figure 5 displays the evolution of the phase-space distribution of interacting atoms in the trap already considered in Figs. 1 and 2. The initial state [Fig. 5(a)] displays strong position-momentum correlations of the atoms, in particular the Wigner function oscillations due to the sharp decrease of the position space wave function, between $x=30$ μm and $x=50$ μm. In Fig. 5(b), after a very short stage of a rapid acceleration at $t=1.3$ ms the momentum distribution has broadened considerably, from less than $0.5\hbar\,\mu\mathrm{m}^{-1}$ to about $2\hbar\,\mu\mathrm{m}^{-1}$ [note the changed momentum scale in Fig. 5(b)], and sheared clockwise. The inner part of the distribution is deformed much stronger, as the spatial gradient, and thus the acceleration is stronger than on the outer wing. Whereas due to the repulsion atoms are accelerated away from the maxima $x=\pm d$, by contrast, atoms approaching the overlap zone $x=0$ are decelerated.

This has to be compared with Fig. 1(b) where, in the *absence* of interactions, both the interference zone and the source zones expand without acceleration, i.e., in the same way. As a consequence, the spatial width of a single condensates extends over nearly 400 μm in Fig. 5(c), i.e., roughly

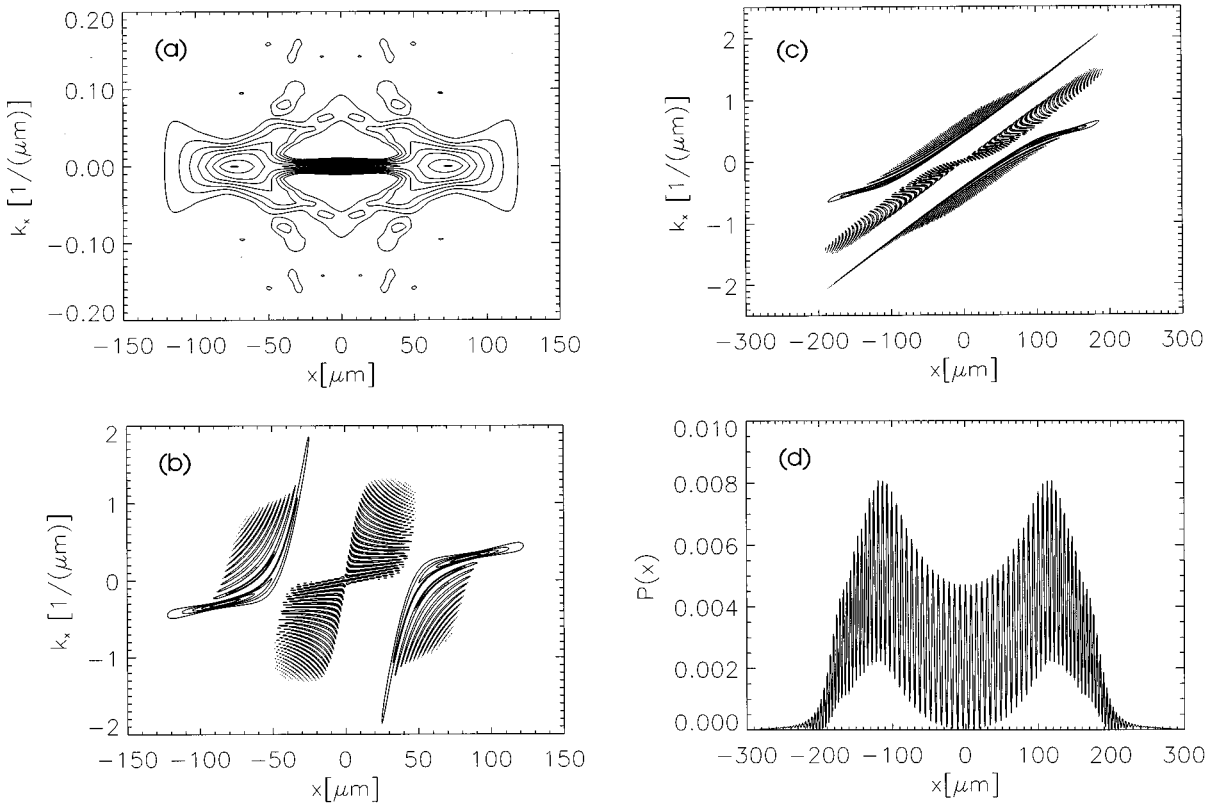

FIG. 5. Wigner function for interacting atoms in phase space, for the same trap parameters as in Fig. 1, but including interactions of $N=5\times10^6$ atoms. (a) Initial state. (b) Early stage of the expansion, $t=1.3$ ms. Note the different momentum scale. (c) $t=38.2$ ms. The interference fringes near $x=0$ are displayed with a much higher amplitude, due to earlier overlap of the density profiles. Spatially resolved fringes are displayed with a very narrow fringe spacing in the position distribution (d), corresponding to (c).

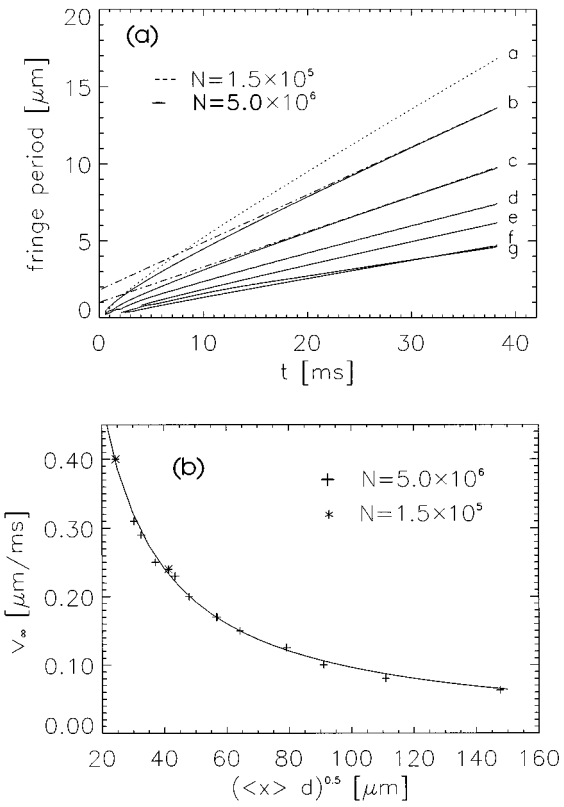

FIG. 6. (a) Time dependence of the width of the central interference fringe. Asymptotic lines are fitted for curves *a* and *b*. The propagation was calculated using the factorized NLSE. For parameters, see Table I. (b) Dependence of asymptotic expansion velocity [slopes of the curves in (a)] on the quantity $\tilde{d}$ from Eq. (3.14).

four times broader than the distribution in Fig. 1(c), for the expansion time $t=38.4$ ms. Thus, due to the above-mentioned rapid acceleration of the atoms, a complete overlap of the condensates has occurred at $t=38.4$ ms, and many more fringes are visible in Fig. 5(d).

For comparison with the noninteracting case, we evaluated the fringe distance as a function of time for different parameters (see Table I). The data displayed in Fig. 6 indeed support the validity of a scaling description of the expansion, for large time. For large light shifts, the shape of the individual condensates is nearly parabolic, and the velocity of expansion of the fringes, as well as the actual fringe spacing at a given time, is inversely proportional to the spacing d. Thus after the initial expansion the dynamics mirrors that of a noninteracting gas. For small light shifts, however, the potential wells are not symmetric with respect to the local minima, and also the position of the minimum does not coincide with the center of gravity of the distribution. In this situation the fringe spacing does not depend on the distance d between the minima, but on a length $\tilde{d}$ characterizing an averaged initial distance between the condensates. The slope of the lines in Fig. 6(a) is evaluated and compared with $\hbar\pi/m\tilde{d}$ [see Fig. 6(b)]. We have found empirically that the modified distance $\tilde{d}$ that allows best for the shifted center of gravity $\langle|x|\rangle=\int_0^\infty x\rho(\mathbf{r})$ of the interacting atoms is given by

$$\tilde{d}=\sqrt{d\langle|x|\rangle}. \tag{3.14}$$

TABLE I. Trap parameters for the divided Ioffe trap, corresponding to curves *a*–*g* in Fig. 6(a). The maximum light shift V_1 is given in frequency units, the laser beam waist in μm.

Curve	w_0 (μm)	$V_1/2\pi\hbar$ (kHz)	N
a	9.3	25	1.5×10^5
b	9.3	25	6×10^6
c	18.3	25	6×10^6
d	30	25	6×10^6
e	30	125	6×10^6
f	30	7000	6×10^6
g	67.2	25	6×10^6

The numerical data for the asymptotic expansion velocity are surprisingly well reproduced by a $1/\tilde{d}$ law, as displayed in Fig. 6(b). Note that this result holds only for the combination of a harmonic potential well with a Gaussian barrier, as in [14].

We finally mention the case of not-well-resolved condensates. For an insufficient light shift or a too large number of atoms, the Thomas-Fermi self-consistent potential does not display a clear potential barrier at $x=0$. In this case the initial density mirrors the total potential, i.e., shows a single two-peaked distribution along z. Also in the case of noninteracting atoms, we find a decreasing number of interference fringes as $d\to\sigma$, and the two sources merge to give a single source. This is in agreement with the conclusion of Sec. II. However, in the case of interacting atoms the condensates expand more rapidly, and more density oscillations show up on the wings of the overlap region after the bulk of the condensates have passed each other.

E. Expansion and interference of a single condensate in a wedge-shaped potential

We finally study the coherent evolution of a single condensate after suddenly switching the potential from a parabolic into a wedge-shaped potential $V=v_0|x|$, where $v_0/2\pi\hbar=40$ Hz μm^{-1}. By temporally switching between different external potentials a single condensate can be turned into a coherently excited superposition state that may split up into two separate parts that recombine later on. The wave-packet dynamics is strongly influenced by the nonlinear dispersion, in the case of interacting atoms. The observation of coherent wave-packet dynamics would also depend on the maintenance of coherence during the observation time.

Quite subtle aspects of the nonlinear dynamics come into play here, which have no classical or quantum mechanical analog. In the initial stage of the expansion, the condensate apparently ''adapts'' its shape to the new potential. An analogous and very fundamental phenomenon has been found in the initial propagation of Gaussian wave packets in nonlinear media. For positive dispersion and negative Kerr coefficient, a (self-attracting) soliton constitutes the fundamental form-invariant propagation mode of the system. For nonsoliton initial wave packets, the different components of the initial wave packet disperse in such a way that asymptotically the self-reproducing soliton survives [17]. The amplitude of the Gaussian that is not contained in this asymp-

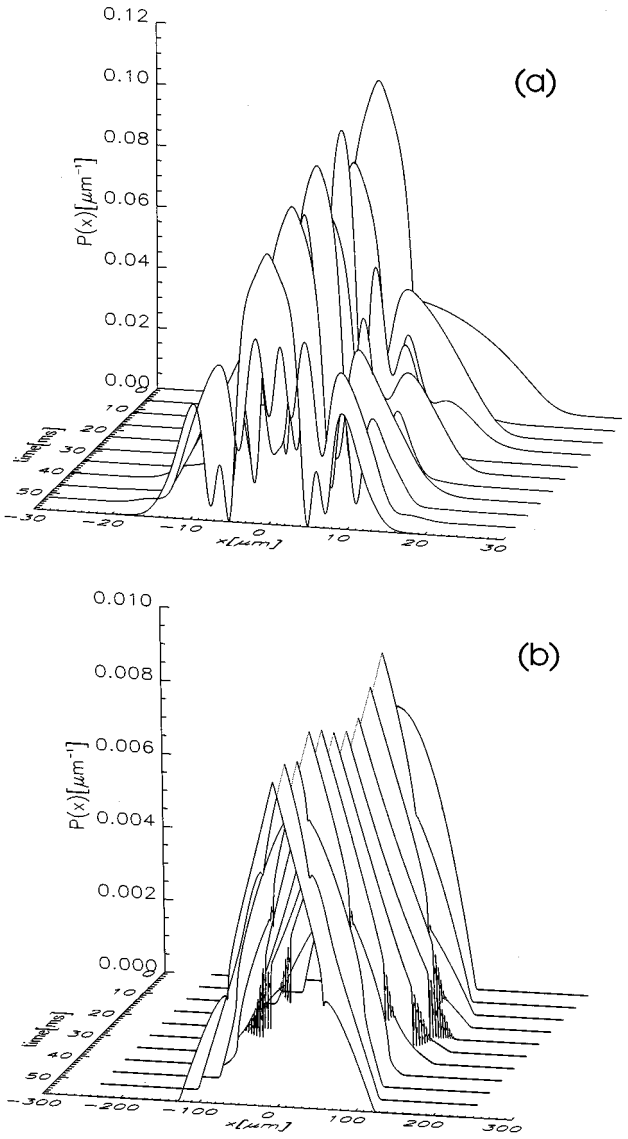

FIG. 7. Expansion and interference after sudden switch to a wedge potential. (a) Solution of NLSE for $N=2400$ atoms. (b) Solution of NLSE for $N=5\times10^6$ atoms.

totical wave packet has been ''radiated'' away, i.e., it has propagated dispersively such that its contribution has become negligible compared to the soliton. It is now interesting to investigate whether similar phenomena are present here.

In the case of the wedge-shaped potential we compare the results for different values of the nonlinearity (atom number). The transverse trapping field is assumed to remain constant such that the nonlinearity does not decrease due to a transverse (y,z) expansion. For small nonlinearity, the amplitude that is propagating outward in the x direction interferes with the amplitude that has been reflected at the linear slope of the potential, resulting in large scale fringes moving in the position space density [Fig. 7(a)]. For high nonlinearity, the wave function of the interacting atoms looks different [Fig. 7(b)]. Initially, the condensate displays a ''creeping'' motion such that the shape of the cloud seems to gradually adapt to the new potential form. This behavior simulates the soliton filter effect mentioned above. However, as the potential rises to infinity, there is no possibility of radiating away the part of the amplitude that does not fit into the self-consistent shape. The reflection at the outer potential slope again creates density oscillations, however, of much reduced period and amplitude. Under suitable conditions the observation of fringes from a single condensate might provide novel evidence for the wave-packet dynamics of a many-particle system.

IV. COLLISIONAL LOSS OF COHERENCE

As mentioned above, all conclusions derived from the NLSE are based on the assumption that the condensate can be described by a single macroscopically occupied one-particle state. However, thermalizing collisions will play a crucial role for long expansion times. Regrettably, no viable theory exists for the treatment of the dynamics of inhomogeneous condensates in such a nonequilibrium situation. In order to obtain a preliminary estimate for the influence of collisions on the interference, we resort to the following considerations, which are based on the homogeneous situation.

The basic assumption of our treatment above is that the macroscopic wave functions of the two independent condensates can be added coherently with an arbitrary but fixed phase Eq. (2.1). The detailed analysis in terms of correlation functions [4] showed that a visible interference between the two condensates requires the criteria Eqs. (4.1) and (4.2) to be fulfilled. The condition

$$\langle a_1^\dagger a_1\rangle \approx \langle a_2^\dagger a_2\rangle \approx N/2 \tag{4.1}$$

implies that the occupation of the two condensate modes $(i=1,2)$ has to be comparable to the total number of atoms N. In addition, N has to be so large that a clearly recognizable spatial pattern can be resolved in a single run of the experiment.

It is not obvious that a condition like Eq. (4.1) will be fulfilled for arbitrary times in the presence of collisions. The equilibrium in free space is characterized by incoherent superpositions of plane waves, to which the initial state cannot evolve by the NLSE. Eventually, thermalizing collisions in the overlap zone will smooth out the momentum distribution. As a result the phase space density might decrease below the degeneracy threshold. However, as mentioned above, a quantitative description of this process is still lacking. We estimated that the collision rates in a thermal cloud with comparable velocity distribution and density would have depleted about half of the condensates in our situation. This would still leave a fringe visibility of about 50%. We expect that this rather overestimates the effect since collisions back into the condensate are favored by the bosonic enhancement factors.

The second condition for visible interference justifies the notion of a broken gauge symmetry in Bose-Einstein condensation, although coherent states do not exist for atoms.

$$\frac{|\langle a_i^\dagger(t)a_i(t+\tau)\rangle|}{\langle a_i^\dagger a_i\rangle} \approx 1. \tag{4.2}$$

It requires that the phase coherence has to be large during the observation time τ, in which the spatial pattern is recorded.

Note that τ refers only to the exposure time and not to the full expansion time that precedes the recording of the pattern.

It turns out that condition (4.2) should be much easier to fulfill, since the relative phase between the condensates needs to be stable only during the exposure time τ of the pattern image, which is normally much shorter than the full expansion time. Therefore, incoherent processes should not be able to violate condition (4.2) as long as they fulfill the much more stringent condition (4.1) on the time scale of the full expansion. However, it has been observed [6,7,16] that even the nondissipative NLSE is able to induce a phase dispersion. The corresponding self-interaction for a single condensate ($i=1,2$) is

$$\mathcal{H}_{\rm int}=\frac{\widetilde{U}}{2V}a_i^\dagger a_i^\dagger a_i a_i . \tag{4.3}$$

In addition, cross coupling terms between the condensates exist, but do not contribute to the phase diffusion. The above Hamiltonian induces phase factors that depend on the actual number of particles in the condensate. Atom number fluctuations thus lead to a phase diffusion since subensembles with a larger atom number exhibit a faster oscillation. The correlation function of condition (4.2) therefore evolves due to

$$\langle a_i^\dagger(t)a_i(t+\tau)\rangle=\sum_{N_i=1}^{\infty}N_iP(N_i)\exp\left(-i\frac{\widetilde{U}}{\hbar V}(N_i-1)\tau\right), \tag{4.4}$$

where $P(N_i)$ is the number distribution for the corresponding condensate. Assuming a Poissonian number distribution $P(N_i)=\exp(-\overline{N_i})\overline{N_i}^{N_i}/N_i!$, this reduces to

$$\begin{aligned}\langle a_i^\dagger(t)a_i(t+\tau)\rangle&=\overline{N_i}\exp(-\overline{N_i})\sum_{N_i=0}^{\infty}\frac{\left[\overline{N_i}\exp\left(-i\frac{\widetilde{U}\tau}{\hbar V}\right)\right]^{N_i}}{N_i!}\\&=\overline{N_i}\exp[\overline{N_i}(e^{-i(\widetilde{U}\tau/\hbar V)}-1)].\end{aligned} \tag{4.5}$$

After an initial decay of the correlation function, revivals [6,7] will be visible after $\tau\approx\hbar V/\widetilde{U}$, which, however, is arbitrarily long in the thermodynamic limit. It is therefore reasonable to expand the second exponential up to second order, thus obtaining

$$\frac{|\langle a_i^\dagger(t)a_i(t+\tau)\rangle|}{\langle a_i^\dagger a_i\rangle}=\exp\left(-\frac{(\overline{n_i}\widetilde{U}\tau)^2}{2\hbar^2\overline{N_i}}\right), \tag{4.6}$$

where we have expressed the quantization volume V by the density $\overline{n_i}$ and the particle number N_i, so as to indicate the proper extension to inhomogeneous situations.

In accordance with the notion of a broken gauge symmetry, the above mechanism of phase diffusion vanishes in the thermodynamic limit. However, in our finite situation, the correlation time would be only somewhat larger than the full expansion time. Since the exposure time τ required to shoot a single picture of the condensate is much shorter, this decorrelation mechanism should not affect the visibility of the fringes.

Therefore, we conclude that the phase decoherence Eq. (4.6) due to the nonlinearity of the Hamiltonian should not inhibit the visibility of the interference. In contrast, the effect of an incoherent depopulation due to collisions might already be detrimental in our situation. It could possibly be overcome by adiabatically widening the trap, before releasing the atoms.

V. CONCLUSION

Summarizing our main results, the mean-field dynamics of expanding Bose condensed clouds, initially at zero temperature, is characterized by the fast transformation of interaction energy into kinetic energy. After this initial stage a free flight stage follows, with the extension of the condensate increasing linearly with time. Interference fringes occur in the overlap region between two expanding atom clouds. The fringe spacing increases linearly in time as well, at a velocity inversely proportional to the initial distance between the condensates. The Wigner representation of the phase space density provides a clear understanding of the condensate dynamics, both in the noninteracting and interacting case, that is not as simply obtained from the position space distributions. It may also allow the problems of spatial and temporal coherence of the condensate to be tackled.

An observation of the predicted interference fringes would unambiguously prove the existence of a quantum mechanical many-particle superposition state. In other words, it is evidence for the macroscopic population of a single atomic center-of-mass quantum state. From calculations of collision rates we have inferred that the decay of the first order coherence function, the ''phase relaxation'' of the condensate wave function, would be slow compared to the interaction time considered here. In the long-time limit, however, collisions between the counterpropagating condensates will increase the phase space volume filled by the condensate, i.e., decrease the phase-space density inevitably.

ACKNOWLEDGMENTS

H.W., A.R., and M.N. thank R. Chiao for fruitful discussions on the properties of solitons. Financial support by the Deutsche Forschungsgemeinschaft (Grants No. Wa 727/4-1 and No. Wa 727/6-1) is acknowledged.

[1] M. H. Anderson, J. R. Ensher, M. R. Matthews, C. E. Wieman, and E. A. Cornell, Science **269**, 198 (1995).

[2] K. B. Davis, M.-O. Mewes, M. R. Andrews, N. J. van Druten, D. S. Durfee, D. M. Kurn, and W. Ketterle, Phys. Rev. Lett. **75**, 3969 (1995).

[3] J. Javanainen and S. M. Yoo, Phys. Rev. Lett. **76**, 161 (1996).

[4] M. Naraschewski, H. Wallis, A. Schenzle, J. I. Cirac, and P. Zoller, Phys. Rev. A **54**, 2185 (1996).

[5] J. I. Cirac, C. W. Gardiner, M. Naraschewski, and P. Zoller, Phys. Rev. A **54**, 3714 (1996).

[6] Y. Castin and J. Dalibard (unpublished).
[7] T. Wong, M. J. Collett, and D. F. Walls, Phys. Rev. A **54**, 3718 (1996).
[8] Y. Kagan, E. L. Surkov, and G. Shlyapnikov, Phys. Rev. A **54**, 1753 (1996).
[9] Y. Castin and R. Dum (unpublished).
[10] M.-O. Mewes, M. R. Andrews, N. J. van Druten, D. S. Durfee, D. M. Kurn, and W. Ketterle, Phys. Rev. Lett. **77**, 416 (1996); M.-O. Mewes, M. R. Andrews, N. J. van Druten, D. M. Kurn, D. S. Durfee, C. G. Townsend, and W. Ketterle, *ibid.* **77**, 988 (1996).
[11] E. Wigner, Phys. Rev. **40**, 749 (1932).
[12] M. Hillery, R. F. O'Connell, M. O. Scully, and E. P. Wigner, Phys. Rep. **106**, 121 (1984).
[13] Second-order terms occur, however, for dissipative systems, describing quantum fluctuations.
[14] W. Ketterle (unpublished).
[15] A. L. Fetter, Phys. Rev. A **53**, 4245 (1996).
[16] M. Lewenstein and L. You, Phys. Rev. Lett. **77**, 3489 (1996).
[17] D. Burak and W. Nasalski, Appl. Opt. **33**, 3969 (1994).